Engineering lytic polysaccharide monooxygenases (LPMOs) for immobilisation on carbon nanotubes

Journal Pre-proofs

Research article

Engineering lytic polysaccharide monooxygenases (LPMOs) for immobilisation on carbon nanotubes

Kelsi R. Hall, Carlotta Pontremoli, Tom Z. Emrich Mills, Fabrizio Careddu, Matteo Bonomo, Claudia Barolo, Vincent G.H. Eijsink, Silvia Bordiga, Morten Sørlie

PII: S0021-9517(25)00173-3
DOI: https://doi.org/10.1016/j.jcat.2025.116108
Reference: YJCAT 116108

To appear in: *Journal of Catalysis*

Received Date: 22 January 2025
Revised Date: 20 March 2025
Accepted Date: 24 March 2025

Please cite this article as: K.R. Hall, C. Pontremoli, T.Z. Emrich Mills, F. Careddu, M. Bonomo, C. Barolo, V.G.H. Eijsink, S. Bordiga, M. Sørlie, Engineering lytic polysaccharide monooxygenases (LPMOs) for immobilisation on carbon nanotubes, *Journal of Catalysis* (2025), doi: https://doi.org/10.1016/j.jcat.2025.116108

Engineering lytic polysaccharide monooxygenases (LPMOs) for immobilisation on carbon nanotubes.

Kelsi R. Hall[1,3]‡, Carlotta Pontremoli[2,]‡ Tom Z. Emrich Mills[1], Fabrizio Careddu[2], Matteo Bonomo[2], Claudia Barolo[2], Vincent G. H. Eijsink[1], Silvia Bordiga[2], and Morten Sørlie.[1*]*

[1] Faculty of Chemistry, Biotechnology and Food Science, Norwegian University of Life Sciences (NMBU), 1432, Ås, Norway.

[2] University of Torino, Department of Chemistry, NIS Interdepartmental Centre and INSTM Reference Centre, Via Quarello 15a, 10135, Turin, Italy.

[3] Biomolecular Interaction Centre and School of Biological Sciences, University of Canterbury, PO Box 4800, Christchurch 8140, New Zealand.

**Correspondence to:

Morten Sørlie (morten.sorlie@nmbu.no)

Claudia Barolo (claudia.barolo@unito.it)

‡ These authors contributed equally to this work.

KEYWORDS (Word Style "BG_Keywords"). Biocatalysis; Lytic polysaccharide monooxygenase (LPMO); Enzyme immobilisation; Multiwalled Carbon Nanotubes; Oxidative damage; cellulose.

ABSTRACT. Lytic polysaccharide monooxygenases (LPMOs) are mononuclear copper-containing enzymes that are able to oxidise C–H bonds in the glycoside linkages of polysaccharides. However, LPMOs are prone to oxidative damage, particularly in the absence of an adequate substrate. In this work, we investigated whether we could immobilise LPMOs and whether such immobilisation could enhance the stability of LPMOs while preserving the essential catalytic properties of the copper active site. Two LPMOs from different families, *Ls*AA9A and *Sc*AA10C, were selected and immobilised on carboxylic acid functionalised multiwalled-CNTs, using a two-step carbodiimide activation reaction. To improve the frequency of enzyme immobilisation and guide site-specific orientation, the enzymes were engineered, introducing two lysine residues on two different loops on the LPMO surface. Assessment of the oxidase and peroxidase activities of the LPMO-MWCNT bioconjugates showed that immobilisation of the engineered LPMO was much more efficient compared to the wild-type enzymes. The immobilised enzymes still showed activity on several substrates, confirming retained catalytic competence following immobilisation. Incubation of the free and immobilised LPMOs under damaging conditions indicated a protective effect of immobilisation for *Ls*AA9A-MWCNT, indicating that, for some LPMOs, immobilisation on MWCNTs may protect against oxidative damage.

Introduction

Lytic polysaccharide monooxygenases (LPMOs) are monocopper enzymes capable of degrading β-1,4-glycosidic bonds in a range of recalcitrant polysaccharides[1-5]. The catalytic activity of these enzymes requires hydrogen peroxide as an oxidant[6] and reducing power to prime the copper, which can be provided in many forms, including small molecular weight reductants like ascorbate[2] and phenolic compounds[7,8], as well as other redox enzymes[4,9,10]. LPMOs have received much attention, not only because of their importance for the efficient bioprocessing of recalcitrant abundant polysaccharides such as cellulose[11,12], but also because of their unique monocopper active site, which has inspired recent work on synthetic small molecule copper catalysts[13,14].

The stability of LPMOs is affected by various well known factors such as pH and temperature, but also, and in particular, by oxidative self-inactivation caused by reactive oxidising species formed at the catalytic centre[6]. Such inactivation is accelerated in the absence of a suitable substrate[15,16]. Oxidative damage to the active site histidine brace[6] can release the bound copper ion into solution, causing a self-inflicted damaging cycle where the released copper promotes high production of hydrogen peroxide through abiotic oxidation of commonly used reductants such as ascorbate, which in turn results in increased LPMO damage[17]. Therefore, the concentrations of reductant, substrate and hydrogen peroxide need to be carefully controlled to ensure a stable and productive enzyme reaction.

To date, one of the most promising and successful strategies to improve enzyme stability is enzyme immobilisation[18]. Immobilisation refers to a procedure where enzymes are stably placed on or within solid supports. The solid support matrix typically enhances the stability of the enzyme by providing protection to environmental changes while preserving activity[19]. Moreover, this approach enables enzymes to be efficiently reused across multiple operational cycles and allows seamless integration into flow bioreactors, enhancing the efficiency of chemical biomanufacturing processes[20,21]. Current immobilisation strategies include both irreversible (*i.e.* covalent immobilisation, cross-linking) and reversible (*i.e*. ionic interaction, adsorption and physical entrapment) techniques. The latter are simple and efficient however result in the formation of relatively weak adducts through intermolecular interactions between the enzyme and the support matrix, which may lead to enzyme leakage from the support. Another issue is the control of the orientation of the enzyme on the support matrix, which will affect access of reactants to the active site. Irreversible methods, such as covalent attachment, are more reliable and controllable. In addition, covalent attachment allows for site-directed immobilisation, which may be important for tuning enzyme selectivity, activity and productivity.

A plethora of support matrices have been used for enzyme immobilisation, including natural polymer-derived carriers (alginate, dextran, chitosan and cellulosic films), synthetic polymers (polypyrrole, polystyrenes and polyvinyl alcohols), inorganic matrices (graphite, carbon black, graphene, carbon nanotubes – CNTs), gold nanostructures and metal oxides[20,22,23]. Among these, CNTs have been widely used as support matrices due to their many desirable properties including high mechanical strength and conductivity, inertness, rapid electron transfer kinetics, and a large surface to volume ratio[24-26].

Here, we addressed if immobilisation can increase the stability of LPMOs while maintaining catalytic features of the copper site. To do so, two LPMOs from different families, *Ls*AA10A and *Sc*AA10C, were immobilised on multiwalled CNTs (MWCNTs) using covalent immobilisation (see scheme 1 in the Materials and Methods section). Enzymes can be immobilized on different supports through several approaches, involving different aminoacidic residues depending on the functional groups available on the support and the selected immobilization strategy. Here, to achieve covalent immobilisation, we utilised carboxylic acid functionalised MWCNTs, allowing for the formation of an amide bond between the COOH moieties of the MWCNTs and amine groups from the enzyme, a technique which has been successfully used for other enzymes[27,28]. In this regard, lysine residues are frequently exploited in enzyme immobilization due to their exposed ε-amino groups, which readily form covalent bonds with activated COOH and epoxy functional groups such as N-hydroxysuccinimide (NHS) esters. To improve the efficiency of enzyme immobilisation and guide site-specific orientation, the two LPMOs were engineered, introducing highly exposed lysine residues on the substrate binding surface, while removing other (partially) exposed lysines.

We report the successful immobilisation of these engineered LPMO variants, which showed improved immobilisation efficiency relative to the wild-type enzymes. We also show retention of catalytic activity and, for one of the enzymes, a decrease in susceptibility to oxidative damage.

Results and Discussion

Preliminary tests: Immobilisation of wild-type LPMOs.

As a first test, appropriate LPMO candidates were selected to be covalently immobilised onto carboxylated (COOH) MWCNTs using lysine residues natively present in the LPMOs. Two LPMOs, *Ls*AA9A (from *Lentinus similis*) and *Sc*AA10C (from *Streptomyces coelicolor*), containing a low number of lysine residues were selected. This opened the possibility to engineer these enzymes by removing the low number of native lysine residues in undesirable positions and introducing novel lysine residues at exposed positions on the substrate binding surface. While this approach could also be attempted for LPMOs containing more native lysine residues, it would require larger amounts of engineering (Figure S1). These two LPMOs were also selected due to their differences in domain structure [*Sc*AA10C contains a carbohydrate-binding domain (CBM), *Ls*AA9A only contains a catalytic domain] and activity (*Ls*AA9A is C1/C4-oxidising LPMO active on both soluble and insoluble substrates, *Sc*AA10C is a C1-oxidising LPMO only active on insoluble substrates), allowing the impact and potential of immobilisation to be assessed for LPMOs with different properties. The method of immobilisation on COOH-MWCNT was modified starting from protocols previously reported in the literature[29,30]. Bovine serum albumin (BSA) was initially selected as control protein while horse radish peroxidase (HRP) was selected as a secondary control. HRP contains significantly less lysine residues than BSA (59/585 = 10.5%, for BSA; 6/306 = 2% for HRP; Figure 1), making it a good mimic for *Ls*AA9A and *Sc*AA10C and allowing the immobilisation procedure to be optimised with a commercially available protein.

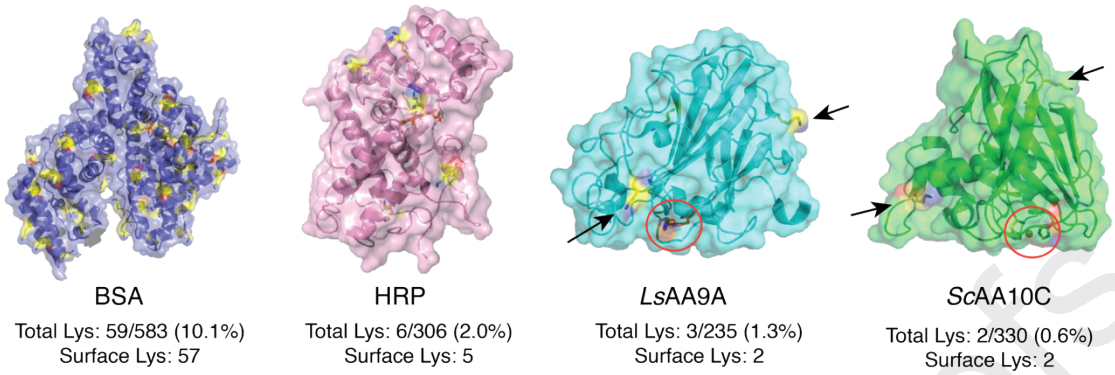

Figure 1. **Candidate proteins for covalent immobilisation using lysine residues**. The lysine residues are shown as sticks with CPK colouring and the carbon atoms coloured in yellow. The copper ion and histidine brace in the LPMOs is indicated by a red circle. A surface view is shown for all proteins, meaning that only fully or partially surface-exposed lysine residues are visible. Total Lys states the number of lysine residues out of the total number of amino acids in the protein. Surface Lys states the number of lysine residues present on the surface of the protein *i.e.* the number of lysine residues available to potentially participate in covalent immobilisation. The two surface-exposed lysine residues present in *Ls*AA9A and *Sc*AA10C are indicated with arrows for clarity. Note that *Sc*AA10C is a two-domain protein for which only the catalytic domain, containing the two lysine residues, is shown.

BSA, HRP, wild-type *Ls*AA9A and *Sc*AA10C were immobilised on carboxylic functionalised multi-walled CNTs (COOH-MWCNTs) using a two-step carbodiimide activation/immobilisation reaction (see Materials and Methods section for details). The reaction was performed using a mass ratio of 1:2.5 (COOH-MWCNT : protein), followed by a dialysis step with a 100 kDa cut off membrane to remove the free protein. This process was successful for the control proteins (BSA and HRP; Figure S2), while no or minimal protein was detected in the case of *Ls*AA9A-MWCNT and *Sc*AA10C-MWCNT samples (Figure S3). This apparent lack of immobilisation of the LPMOs is further supported by the absence of catalytic activity (Figure S3). This unsuccessful immobilisation may be ascribed to the limited number of lysine residues on the surface of *Ls*AA9A and *Sc*AA10C, combined with their location and their limited degree of surface exposure.

Engineering LPMOs for immobilisation.

The canonical LPMO structure consists of an immunoglobin-like β-sandwich core structure. Structural diversity primarily comes from loops that connect the β-strands, and these loops contribute to shaping the substrate-binding surface of LPMOs[31]. Consequently, numerous loops are present on the LPMO surface, offering target sites for mutagenesis. Lysine residues were introduced into such surface loops in *Ls*AA9A and *Sc*AA10C, through site-directed mutagenesis. To increase the chances of successful immobilisation, two lysine residues were introduced targeting two loops in each of the LPMOs (Figure 2). At the same time, the two naturally occurring

lysines close to the surface were also mutated in each of the two proteins, thus directing immobilisation to the highly surface-exposed lysine residues that were introduced (See Materials and Methods section for details). The engineered *Ls*AA9A (*Ls*AA9A_v2) and *Sc*AA10C (*Sc*AA10C_v2) variants were well expressed and were, after purification and copper saturation, immobilised onto COOH-MWCNTs using the same weight ratio (1:2.5 MWCNT: protein) previously employed for the wild-type LPMOs, BSA and HRP. We estimated the immobilisation reaction efficiency as the amount of immobilised protein relative to the amount of protein added in the immobilisation reaction. To do this, the protein content of the LPMO_v2-MWCNTs samples was assessed using SDS-PAGE using ImageJ[32] to quantify the protein bands against a standard curve created with free enzyme. This revealed the successful immobilisation of both *Ls*AA9A_v2 (62%, corresponding to 0.39 mg/mL) and *Sc*AA10C_v2 (20%, corresponding to 0.12 mg/mL) (Figure 2). This implies that suspensions of LPMO_v2-MWCNTs containing 0.25 mg/mL of MWCNs, have molar LPMO concentrations of 15.5 mM and 3.5 mM, for the *Ls*AA9A and the *Sc*AA10C bioconjugates, respectively.

The estimated LPMO concentrations would imply that about 9.3×10^{15} (*Ls*AA9A) and 2.1×10^{15} (*Sc*AA10C) LPMO molecules are bound per 0.25 mg of MWCNT, which supposedly contain at least 2.7×10^{17} COOH moieties (> 8% w/w, as reported by the supplier). This would imply that LPMOs are linked to approximately 1 – 4 % of the originally available COOH groups.

Note that, in this proof-of-concept study, no attempts were made to optimise these reaction efficiencies, for example by varying the MWCNT-LPMO weight ratio during the immobilisation reaction. It should be noted that traditional protein quantification methods (*i.e.* absorbance at 280 nm or a Bradford protein assay) could not be used to estimate the protein content of the bioconjugates due to the dark colour and low solubility of the MWCNTs. We did however note an increase in the solubility of the MWCNTs following immobilisation, allowing the activity of the bioconjugates to be measured when diluted at an appropriate level.

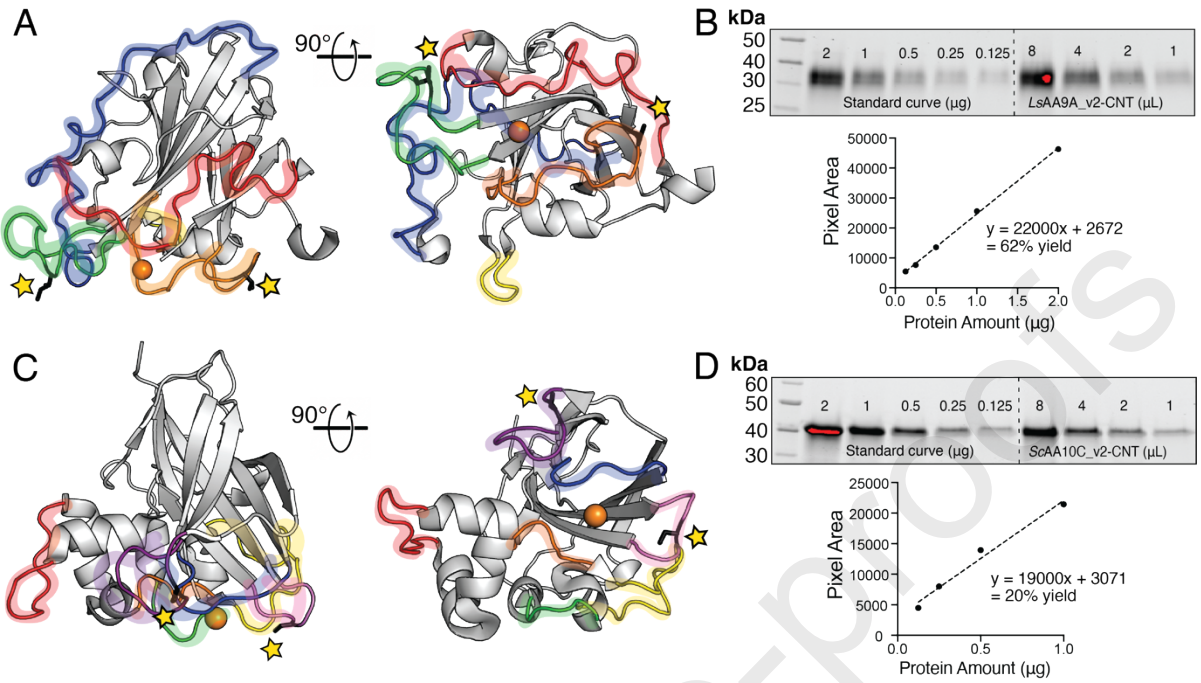

Figure 2. Engineering lysine residues in *Ls*AA9A and *Sc*AA10C and immobilisation of the mutants. Panels A and C show the three-dimensional structures of *Ls*AA9A (A; PDB: 5NLS) and *Sc*AA10C (C; PDB: 4OY7), in two different orientations. Loop regions that contribute to the substrate binding surface of the LPMO are coloured while the remaining structure is shown in grey and the bound copper ion in orange. The side chains of residues that were replaced by lysine are shown as black sticks and are indicated by a yellow star for clarity (*Ls*AA9A: lysine residues introduced in the orange (residues 66-81) and green (residues 147-161), T68K/I158K; *Sc*AA10C: lysine residues introduced in the purple (residues 147-154) and pink (residues 179-183) loops, S182K/S215K). Panels B and C show the protein content of dialysed *Ls*AA9A_v2-MWCNT (B) and *Sc*AA10C_v2-MWCNT (D). To quantify the amount of protein and estimate the reaction efficiency, a standard curve was created using free LPMO (0.125-2 µg of free *Sc*AA10C_v2 or *Ls*AA9A_v2). Areas of oversaturation are shown in red and bands containing such areas were excluded from any calculations. 1 mL of MWCNT sample corresponds to 0.25 mg CNT and 0.625 mg of protein present at the beginning of the immobilisation reaction prior to dialysis.

Assessing the activity of the bioconjugates.

The catalytic activity of the bioconjugates was assessed by diluting the samples 15-fold, to prevent interference from high amounts of MWCNTs in suspension with analytical methods. Activity assays were performed using equivalent amounts of MWCNT-conjugated enzyme or free enzyme (approximately 1.03 µM for *Ls*AA9A_v2 and 0.23 µM for *Sc*AA10C_v2 as estimated by SDS-PAGE). For comparison, free and MWCNT-conjugated WT LPMOs were also included in the assays, using the same WT LPMO concentration for the free enzymes and the same dilution for the WT LPMO-loaded MWCNTs (15-fold). Of note, since minimal protein was detected in the MWCNT-WT LPMO samples (Figure S3A), the actual LPMO concentration in the reactions with

WT LPMO bioconjugates was much lower compared to the reactions with the LPMO_v2 bioconjugates.

One common method for detection of LPMO activity is measuring the oxidase activity of these enzymes, i.e., the ability to generate hydrogen peroxide. In the presence of a reductant, such as ascorbate, the LPMO can convert molecular oxygen to hydrogen peroxide. This is commonly measured using a modified Amplex Red and horse radish peroxidase (HRP) assay[33,34], whereby hydrogen peroxide produced by the LPMO is consumed by HRP to generate a coloured substance, allowing measurements in real time using a simple spectroscopic assay. The oxidase activities of *Ls*AA9A and *Sc*AA10C have been previously measured using this assay, showing that hydrogen peroxide production by *Ls*AA9A[35] is considerably faster than hydrogen peroxide production by *Sc*AA10C[17]. Reliable detection of hydrogen peroxide production for the *Sc*AA10C bioconjugates was impossible, due to the low levels of produced hydrogen peroxide and the background absorbance and scattering caused by the MWCNTs, and is therefore not reported. For the *Ls*AA9A bioconjugates, a low level of activity was detected for WT *Ls*AA9A-MWCNT (Figure 3A), confirming that only a minute amount of protein had been immobilised (Figure S3). In contrast, the *Ls*AA9A_v2-MWCNT bioconjugate showed high oxidase activity on par with the activity of the free enzyme, showing that the immobilised enzyme is active.

An alternative spectroscopic assay for rapid detection of LPMO activity is based on measuring the oxidation of 2,6-dimethoxyphenol (2,6-DMP). This assay measures the peroxidase activity of the LPMO, which is reduced by 2,6-DMP and reoxidised, in a peroxidase reaction, by H_2O_2. This reaction leads to the formation of coerulignone whose absorption can be measured spectrophotometrically at 469 nm[36]. It has been previously observed that there is an inverse relationship between the oxidase and peroxidase activities of LPMOs[37], meaning that this assay could provide reliable information regarding the activity of the *Sc*AA10C variants, with low oxidase activities. While no activity was detected for the WT *Sc*AA10C-MWCNT sample, confirming a lack of immobilisation, clear activity, close to that of the free enzyme, was detected for the *Sc*AA10C-v2-MWCNT sample (Figure 3B). Following the inverse relationship between the oxidase and peroxidase activity, *Ls*AA9A was less active in the 2,6-DMP assay (approximately 5-fold less; Figure 3). However, the method was still suitable for detecting active LPMO giving trends comparable to those obtained when measuring the oxidase activity (Figure 3A). Taken together, the data presented in Figure 3 clearly show that the two immobilised LPMO_v2 have activities similar to those of the free mutant enzymes. Of note, while the oxidase assay could be confounded by free copper leaking from the LPMOs[38,39], excess copper does not affect the 2,6-DMP assay[36].

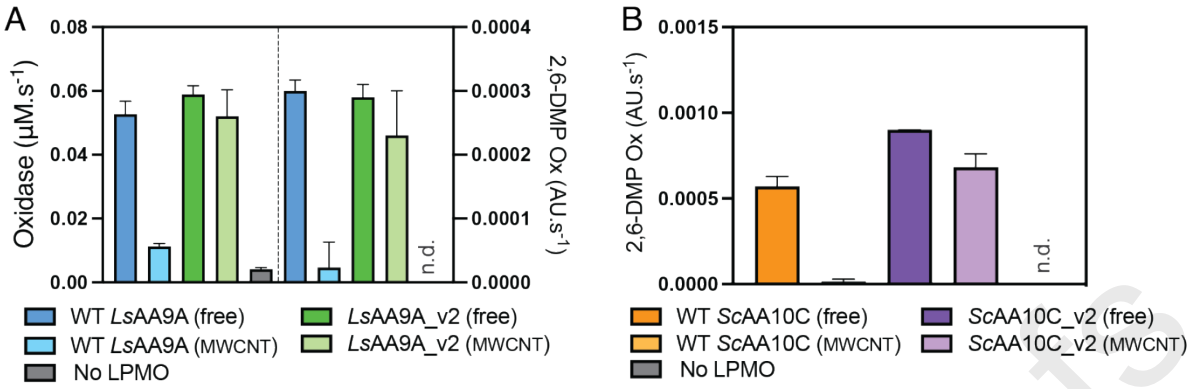

Figure 3. Activity of free and immobilised *Ls*AA9A and *Sc*AA10C, in an oxidase and a peroxidase (2,6-DMP) assay. (A) Activity of WT *Ls*AA9A (blue) and *Ls*AA9A_v2 (green) in the free (dark colour) and the immobilised (light colour) state in the oxidase assay (left-hand Y-axis) and peroxidase (2,6-DMP) assay (right-hand Y-axis). (B) Activity of WT *Sc*AA10C (orange) and *Sc*AA10C_v2 (purple) in the free (dark colour) and immobilised (light colour) state in the peroxidase (2,6-DMP) assay. Oxidase assays, done with *Ls*AA9A only, contained 100 μM Amplex Red, 5 U/mL HRP, 1 mM ascorbate, 50 mM Bis-Tris, pH 6.5, and an amount of bioconjugate or free LPMO corresponding to a final enzyme concentration in the order of 1.03 μM. The reaction was incubated at 30 °C and hydrogen peroxide formation was monitored over time. Peroxidase (2,6-DMP oxidation) reactions contained 1 mM 2,6-DMP, 100 μM hydrogen peroxide, 50 mM Bis-Tris, pH 6.5 (*Ls*AA9A samples), or 50 mM Tris-HCl, pH 7.5 (*Sc*AA10C samples), and an amount of bioconjugate or free LPMO corresponding to a final enzyme concentration of 1.03 μM for *Ls*AA9A variants and 0.23 μM for *Sc*AA10C variants. The reaction was incubated at 30 °C and 2,6-DMP oxidation was monitored over time. Note that the given approximate enzyme concentrations do not apply for reactions with WT enzymes conjugated to MWCNTs; in these reactions, enzyme concentrations were negligible as shown in Figure S3A (see text for details). Error bars show standard deviations for three independent reactions (n = 3). Negative controls are shown in grey (no LPMO). N.d. means a rate could not be determined. Note the changes in Y-axis scales between A and B.

Next, the activity of the bioconjugates on natural substrates was evaluated. Determining oxidised product formation could potentially give insight into the type of immobilisation that had occurred, since it is conceivable that the active site is obscured by the MWCNT, with possible repercussions for the activity on large insoluble substrates. The activity assays were done under *in situ* H_2O_2 limiting conditions, which means that the reaction is limited by generation of the co-substrate H_2O_2 through enzymatic and abiotic oxidation of the reductant. Importantly, the surface mutations may have changed both substrate-binding affinities and modes, as well as the oxidase activity of the LPMOs (Figure 3), which may affect not only productive but also enzyme-inactivating non-productive reactions. Therefore, differences between the wild-type and the mutant enzymes are conceivable.

Activity of the *Ls*AA9A variants was evaluated with both a soluble (cellopentaose) and an insoluble substrate (phosphoric acid swollen cellulose; PASC), measuring the release of C4-

oxidised products over time. Interestingly, regardless of immobilisation, *Ls*AA9A_v2 showed higher initial activity compared to WT *Ls*AA9A (Figure 4A and B). Compared to the free enzyme control reactions, minimal activity was observed for the WT *Ls*AA9A-MWCNT sample acting on cellopentaose or PASC (Figure 4A and 4B), confirming the negligible immobilisation. In contrast, almost identical activities were observed for free and immobilised *Ls*AA9A_v2 on both cellopentaose and PASC (Figure 4A and 4B). The ability of immobilised *Ls*AA9A_v2 to oxidise the insoluble substrate PASC suggests that the substrate binding surface has not been obscured by the MWCNTs, indicating that immobilisation may have occurred via only one of the two lysine residues. PASC is a relatively amorphous substrate and may be relatively easy for an immobilised LPMO to access. Reactions with a more crystalline substrate, Avicel, showed a notable decrease in both the initial rate of the reaction and the total amount of oxidised product released for immobilised *Ls*AA9A_v2 compared to free *Ls*AA9A_v2 (Figure S4). Thus, immobilisation has to some extent reduced the ability of *Ls*AA9A_v2 to interact productively with crystalline substrates.

As far as the *Sc*AA10C variants are concerned, none of the *Sc*AA10C variants showed activity on cellopentaose (Figure S5). Assessment of the *Sc*AA10C variants with PASC, measuring formation of C1-oxidised products over time, showed similar activities for the free and immobilised *Sc*AA10C_v2 samples, confirming that the activity of the enzyme is maintained after the immobilisation. Under turnover conditions, this mutant was less stable than the wild-type enzyme, which translated to lower total released oxidised product (Figure 4C; note that the initial rates of the reactions are the same). A decrease in the stability could indicate that the introduced lysine mutations have affected substrate binding, and in turn, protein stability. Minimal product formation was observed for immobilised WT *Sc*AA10C, confirming the negligible immobilisation of this enzyme. In this case, the free and immobilised mutant enzyme (*Sc*AA10C_v2) showed similar activities on Avicel (Figure S4), which may indicate that immobilisation had occurred on a single lysine residue leaving the immobilised enzyme free to interact with a larger crystalline insoluble substrate.

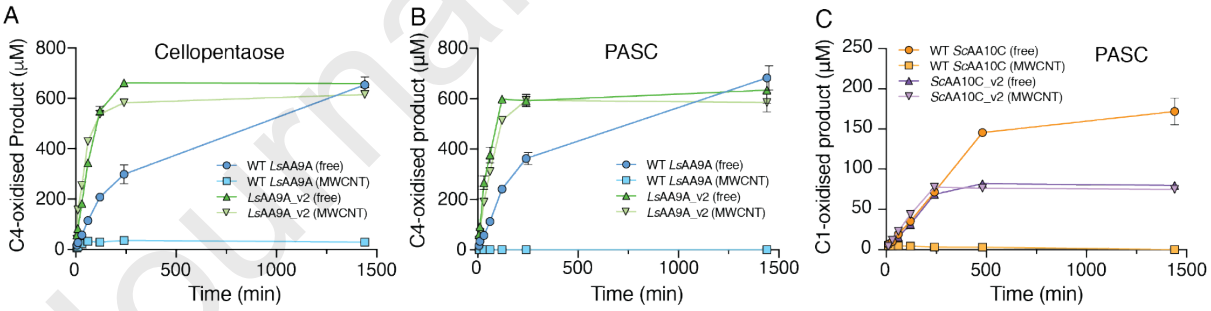

Figure 4. Generation of oxidised products during degradation of cellulosic substrates by free and immobilised LPMOs. *Ls*AA9A variants were tested with (A) cellopentaose and (B) PASC and the reactions contained 1 mM cellopentaose or 0.1% (w/v) PASC, 1 mM ascorbate, 50 mM Bis-Tris, pH 6.5, and an amount of bioconjugate or free *Ls*AA9A variant corresponding to a final enzyme concentration of 1.03 µM. The reactions were incubated at 37 °C and 1000 rpm and sampled over time. *Sc*AA10C variants were tested with (C) PASC and the reactions contained 0.1 % (w/v) PASC, 1 mM ascorbate, 50 mM Tris-HCl, pH 7.5, and an amount of bioconjugate or free *Sc*AA10C variant corresponding to a final enzyme concentration of 0.23 µM. The reactions were incubated at 40 °C, 1000 rpm, and sampled over time. All reactions were performed in the presence

of oxygen and external reductant (AscA) with no exogenous hydrogen peroxide. Error bars show standard deviations for three independent reactions (n = 3). All negative control reactions, *i.e.* reactions with no AscA, showed negligible amounts of oxidised products.

Protective effects of enzyme immobilisation.

A potential benefit of immobilising LPMOs on a MWCNT surface is to protect the LPMO from oxidative damage. It is well-known that LPMOs are sensitive to oxidative damage in the catalytic centre, particularly in the absence of a suitable substrate[6,17]. We considered that the MWCNTs could act like a "substrate" and thus protect the LPMO active site from oxidative damage. To assess this, the mutated LPMOs (free and immobilised) were incubated with ascorbate for various amounts of time in the absence of a substrate, after which residual activity was measured. The results demonstrated how damaging these conditions can be, as in both free mutant LPMOs, inactivation was already evident after only 10 minutes (Figure 5). A stabilising effect of immobilisation was detectable for *Ls*AA9A_v2, showing 20% residual activity after 20 minutes for the free enzyme, compared to around 70% residual activity for the immobilised enzyme (Figure 5A). While this suggests a stabilising effect of immobilisation, such an effect was not observed for *Sc*AA10C_v2 (Figure 5B).

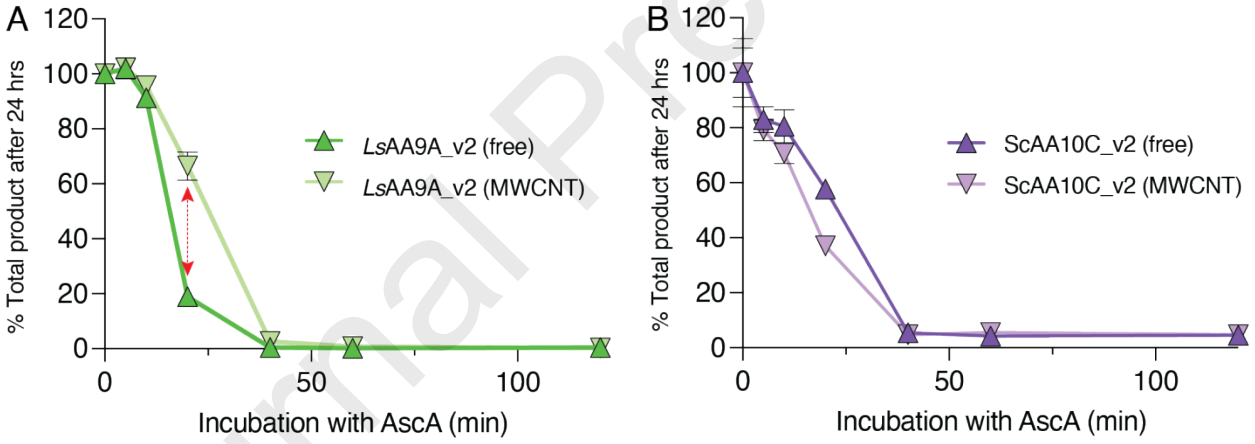

Figure 5. Oxidative damage and residual activity of *Ls*AA9A_v2 and *Sc*AA10C_v2. Oxidative damage was induced by incubating (A) *Ls*AA9A _v2 or (B) *Sc*AA10C_v2 with ascorbate (AscA) in the absence of substrate for a given time-period. Residual activity was monitored by measuring the amount of oxidised product released by the LPMO during a subsequent 24-hour incubation with 1 mM freshly added ascorbate and substrate. The "% Total product after 24 hrs" was determined as: (total amount of oxidised product AscA-preincubated LPMO/total amount of oxidised product not pre-incubated LPMO × 100). The red arrow indicates a conspicuous difference between free and immobilised *Ls*AA9A_v2 samples. The pre-incubation reactions contained 1 mM ascorbate, 50 mM Bis-Tris, pH 6.5 for *Ls*AA9A_v2 and 50 mM Tris HCl pH 7.5 for *Sc*AA10C_v2, and an amount of bioconjugate or free LPMO corresponding to a final enzyme concentration of 1.03 µM for *Ls*AA9A_v2 and 0.23 µM for *Sc*AA10C_v2. The reactions were incubated for various time periods at 37 °C, 1000 rpm, for *Ls*AA9A_v2 samples and 40 °C, 1000 rpm for *Sc*AA10C_v2 samples. Following pre-incubation, 1 mM cellopentaose (*Ls*AA9A_v2

samples) or 0.1% (w/v) PASC (*Sc*AA10C_v2 samples) and an additional 1 mM ascorbate were added to the reactions and the total amount of soluble oxidised products were determined after 24-hours. Error bars show standard deviations for three independent reactions (n = 3).

Conclusions

Here we report a successful immobilisation of engineered LPMOs on COOH functionalised MWCNTs. The immobilisation relies on the introduction of highly exposed lysine residues on the binding surface of the LPMO to efficiently generate covalent bonds with COOH functional groups on the MWCNTs. The obtained immobilisation efficiencies indicate that the loop regions on the binding surfaces of LPMOs are appropriate targets for immobilisation approaches. Importantly, the immobilised LPMOs maintained their oxidase and peroxidase activity, showing activity levels similar to their non-immobilised counterparts. Moreover, for *Ls*AA9A_v2, immobilisation led to higher stability under damaging conditions.

We observed a higher immobilisation efficiency in *Ls*AA9A_v2 compared to *Sc*AA10C_v2, and there are several factors that may affect this efficiency including position of the lysine residues, glycosylation effects, and presence or absence of a carbohydrate binding domain (CBM). While *Ls*AA9A_v2 contains 3 potential N-glycosylation sites and 3 potential *O*-glycosylation sites, these are not predicted to interfere with the immobilisation reaction but is something to consider when selecting LPMOs for this application. The presence or absence of a CBM is also an important factor to consider as it could cause steric hindrance with the MWCNTs. While *Sc*AA10C_v2 (contains a CBM) exhibited a lower immobilisation efficiency than *Ls*AA9A_v2 (no CBM), further experiments would be required to confirm whether this decrease in efficiency was due to the CBM or the LPMO itself. It is important to note here that the *Sc*AA0C CBM does not contain any lysine residues that would interfere with immobilisation.

Although reduced activity could be expected, due to the confinement of the active site, the immobilised enzymes still showed activity on polymeric substrates, confirming the catalytic competence of the immobilised LPMOs. These results likely indicate that immobilisation happened through only one lysine, at least for a fraction of the immobilised enzymes, which would leave considerable flexibility for the enzyme to interact with various substrates. It should also be noted that the activity assays run in this study are primarily limited by the rate of *in situ* production of H_2O_2, which means that variations in the true enzymatic peroxygenase activity may remain undetected. Further kinetic studies with exogenously added H_2O_2, thus monitoring the true peroxygenase activity of the enzymes could be done to provide additional insight into the properties of the immobilised enzymes.

When using the most crystalline of the tested substrates, Avicel, some reduction in activity upon immobilisation was indeed observed for *Ls*AA9A_v2, suggesting that immobilisation did lead to hampered binding of this large and insoluble substrate. Possible steric effects of immobilisation may be further manipulated by using linkers of different lengths or compositions, thus altering the space between the MWCNT surface and the enzyme, or by changing the position and the number of exposed lysines on the protein. The present proof-of-concept study presents an encouraging avenue for future research on the immobilisation of LPMOs.

Experimental section

Site directed mutagenesis and cloning. An AA9 and AA10 LPMO were selected containing a limited number of native lysine residues. Two lysine residues were introduced onto loops present on the surface of *Ls*AA9A (T68K/I158K) and *Sc*AA10C (S182K/S215K). Highly exposed residues on the presumed substrate-binding surface of the LPMOs were selected, while avoiding residues that could affect the catalytic machinery of the enzyme, as well as glycine and proline residues, due the putative impact of these residues on main chain conformation and flexibility. Native lysine residues present on the LPMO surface were selected for mutation based on visual inspection of the proteins and analyses of potential steric clashes using PyMOL (*Ls*AA9A; K32T/K50Q and *Sc*AA10C; K54R/K154R). The native lysine residue at position 100 in *Ls*AA9A was not mutated as it is buried and therefore would not participate in the immobilisation. The generated variants are referred to as "*Ls*AA9A_v2" (K32T/K50Q/ T68K/I158K) and "*Sc*AA10C_v2" (K54R/K154R/S182K/S215K) throughout this paper. Gene fragments encoding these variants were ordered from Thermo Fisher Scientific (Waltham, MA, USA) using codon optimised WT *Ls*AA9A (AN: ALN96977;[40]) and WT *Sc*AA10C (AN: Q9RJY2;[41]) as a starting point. *Ls*AA9A_v2 was cloned into the pBSYGCW14 vector, fusing the protein-encoding gene to the Ost1 signal peptide and *Sc*AA10C_v2 was cloned into the pRSETB vector containing the CBP21 signal peptide. The construct containing the fungal protein (pBSYGCW14_*Ls*AA9A_v2) was used to transform *Pichia pastoris* BSYBG11 and the construct containing the bacterial protein (pRSETB_*Sc*AA10C_v2) was used to transform *Escherichia coli* BL21 (DE3).

Protein expression, purification, and copper saturation. The previously generated *P. pastoris* strain constitutively expressing full-length WT *Ls*AA9A[40] or the newly generated strain expressing *Ls*AA9A_v2 were used to inoculate 2 × 500 mL YPD medium [1% (w/v) yeast extract, 2% (w/v) peptone and 0.2% (w/v) dextrose]. The culture was incubated at 28 °C, 200 rpm for 60 hours. Following incubation, the cells were harvested by centrifugation and the protein containing supernatant was filtered through a 0.22 µm Steritop filter (Merck Millipore, Burlington, MA, USA). Prior to purification, the supernatant was concentrated 10-fold using a VivaFlow 200 tangential flow filtration system with a molecular weight cut-off (MWCO) of 10 kDa (Satorius, Göttingen, Germany). A two-step purification was performed consisting of hydrophobic interaction chromatography (HIC) and size exclusion chromatography (SEC). For HIC, a 5 mL HiTrap Phenyl FF column (Cytiva, Marlborough, MA, USA) was used, which was equilibrated with 50 mM Bis-Tris, pH 6.5, 2.4 M ammonium sulphate. The protein-containing supernatant was adjusted by the addition of ammonium sulphate to a final concentration of 2.4 M and loaded onto the column. Elution of the protein was achieved by applying a linear gradient of 0-100% 50 mM Bis-Tris, pH 6.5, over 40 mL at a flow rate of 2 mL/min. Protein purity was assessed by SDS PAGE and the protein-containing fractions were pooled and concentrated to 1 mL using an Amicon Ultra-15 10 kDa MWCO centrifugal filter unit (Merck Millipore, Burlington, MA, USA). For SEC, a HiLoad 16/60 Superdex 75 size exclusion column (Cytiva, Marlborough, MA, USA) was used equilibrated with 50 mM Bis-Tris, pH 6.5, 200 mM NaCl. The protein was loaded onto the column at a flow rate of 1 mL/min and the protein began to elute after approximately 60 minutes. Protein purity was assessed with SDS-PAGE, and the protein-containing fractions were pooled and concentrated.

The previously generated *E. coli* BL21 (DE3) strain constitutively expressing full-length WT *Sc*AA10C[42] or the newly generated strain expressing *Sc*AA10C_v2 were used to inoculate 2 × 500

mL terrific broth (TB) medium [2.4% (w/v) yeast extract, 2% (w/v) tryptone and 0.4% (w/v) glycerol, 0.017 M KH_2PO_4 and 0.072 M K_2PO_4] supplemented with 100 μg/mL ampillicin. The culture was incubated at 37 °C for 16 hours in a homemade aeration system which utilises compressed air for aeration. The cells were harvested by centrifugation and periplasmic extracts were produced by applying osmotic shock as previously described[43]. The resulting extract was filtered through a 0.22 μm Steritop filter (Merck Millipore, Burlington, MA, USA). A two-step purification was performed consisting of anion exchange chromatography (AEX) and size exclusion chromatography (SEC). For AEX, a 4 mL HiTrap DEAE FF column (Cytiva, Marlborough, MA, USA) was used, which was equilibrated with 50 mM Tris-HCl, pH 7.5. The protein-containing periplasmic extract was loaded directly onto the column. Elution of the protein was achieved by applying a linear gradient from 0 to 50% 50 mM Tris-HCl, pH 7.5, 1 M NaCl over 100 minutes at a flow rate of 3 mL/min. Protein purity was assessed by SDS-PAGE and the protein-containing fractions were pooled and concentrated to 1 mL using an Amicon Ultra-15 10 kDa MWCO centrifugal filter unit (Merck Millipore, Burlington, MA, USA). SEC and subsequent concentration of pure protein were performed as described above using 50 mM Tris-HCl, pH 7.5, 200 mM NaCl as the buffer.

To copper saturate the LPMOs, a 3-fold molar excess of $Cu(II)SO_4$ was added to the pooled and concentrated protein samples, followed by incubation on ice for 60 minutes. Excess of copper and salt was removed, and the protein was simultaneously exchanged into 50 mM Bis-Tris, pH 6.5, (*Ls*AA9A samples) or 50 mM Tris-HCl, pH 7.5, (*Sc*AA10C samples) using an Amicon Ultra-15 Centrifugal filter (Merck, Burlington, MA) with a 10 kDa cut off (minimal dilution factor of the starting buffer was 1×10^6-fold). The final protein concentrations were determined by measuring the A_{280} and using the theoretical extinction coefficients calculated using the ExPASy ProtParam tool[44].

Immobilisation protocol. The immobilisation protocol (shown in scheme 1) was optimised from Jiang *et al.,* (2004)[30] and Alagöz *et al.,* (2021)[29], using multi-walled carboxylic acid functionalised MWCNTs (COOH-MWCNT; >8% carboxylic acid functionalised with an average diameter of 9.5 nm × 1.5 μm; Sigma-Aldrich, St Louis, MO). A first protocol was optimised with WT *Ls*AA9A and WT *Sc*AA10C. To activate the carboxylic groups on the MWCNT surface, 2 mg of COOH-MWCNT was suspended in 1 mL 50 mM Tris-HCl, pH 7.5. Then, 0.5 mL of this suspension was mixed with 0.5 mL of N-Hydroxysuccinimide (NHS, 98%, Sigma Aldrich, St Louis, MO) (37 mg/mL in 50 mM MES, pH 6.1) obtaining a final concentration of 1 mg/mL MWCNT in buffer. This sample was then sonicated (Output 45kHz, 120W) for 10 minutes at room temperature by using an ultrasonic bath USC 600 TH (VWR international, United Kingdom). 2.2 mg of N-(3-dimethylaminopropil)-N′-ethylcarbodiimide hydrochloride (EDC; >98%, TCI Europe) was added to the suspension followed by sonication at room temperature for 2 hours. The suspension was then centrifuged at 11,000 × g and the excess NHS and EDC was removed by washing twice with distilled water. Finally, the MWCNTs were resuspended in 1 mL buffer (50 mM Tris-HCl, pH 7.5, for *Sc*AA10C variants and 50 mM Bis-Tris, pH 6.5, for *Ls*AA9A variants). 2.5 mg of the protein to be immobilised (WT *Ls*AA9A and WT *Sc*AA10C) was added to 1 mL of the activated MWCNTs (corresponding to 1 mg of activated MWCNTs) giving a weight ratio of 1:2.5 (MWCNT: protein). The mixture was stirred at 450 rpm overnight at room temperature. To remove unbound protein the samples were dialysed in the appropriate buffer using a SpectraPor Float-A-Lyzer device with a 100 kDa molecular weight cut off (MWCO) (Repligen, Waltham, MA, USA).

For the immobilisation of BSA, HRP, *Ls*AA9A_v2 and *Sc*AA10C_v2, we used a diluted solution of activated MWCNT resulting in a final concentration of 0.25 mg/mL. Consequently, to maintain the weight ratio of 1:2.5 (MWCNT: protein), 0.625 mg of the protein to be immobilised (BSA, HRP, *Ls*AA9A_v2 and *Sc*AA10C_v2) was added to 1 mL of the activated MWCNTs suspension followed by stirring at 450 rpm overnight at room temperature.

In addition, for the *Ls*AA9A_v2 and *Sc*AA10C_v2 mutants, to prevent any potential oxidative damage during the immobilisation process, the reaction with MWCNTs was performed under nitrogen atmosphere. Specifically, after the activation of the COOH-MWCNTs, the pellets were resuspended in 1 mL of 50 mM Tris-HCl buffer, pH 7.5, or 50 mM Bis-Tris, pH 6.5. Then the suspension of activated MWCNT was purged for 10 minutes with N_2 to remove oxygen from the suspensions.

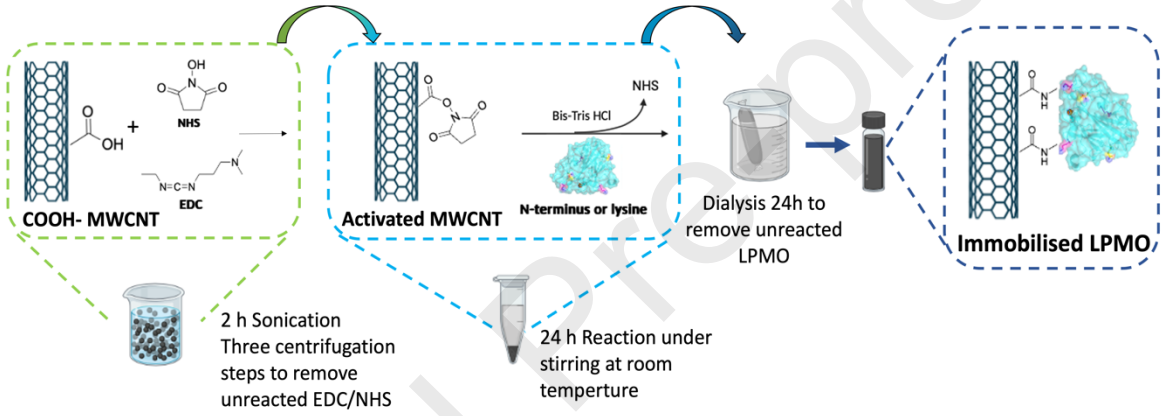

Scheme 1. Protocol for immobilising LPMOs on the surface of COOH-functionalised MWCNTs. The immobilisation protocol involved a two-step carbodiimide activation reaction to activate carboxylic acid functionalised multiwalled-CNTs (COOH-MWCNT). The activated MWCNTs were then mixed with the enzymes and dialysed to obtain the final immobilised LMPO on the COOH-MWCNTs.

Quantification of immobilised enzyme. The amount of immobilised enzyme was evaluated using SDS-PAGE analysis. Four different volumes (1, 2, 4 and 8 µL) of the MWCNT suspensions were mixed with SDS-PAGE sample buffer containing the reducing agent dithiothreitol (DTT) and incubated at 95 °C for 10 minutes to denature the enzyme. The resulting samples were loaded onto a reducing AnykD Mini-PROTEAN TGX Stain-Free gel (Bio-Rad, Hercules, CA, USA). For each LPMO, a standard curve (0.125-2 µg) containing free enzyme was prepared in the same manner. ImageJ[32] was used to quantify the amount of protein present in the standard curve samples and the amount of protein present in the bioconjugates following immobilisation and dialysis.

Oxidase activity. Hydrogen peroxide production by the LPMO was measured using a modified Amplex Red/horse radish peroxidase (HRP) assay[33]. Stock solutions of Amplex Red (10 mM)

were prepared in DMSO. A reaction mixture was prepared containing 100 μM Amplex Red, 5 U/mL HRP (Sigma-Aldrich, St Louis, MO) and an amount of bioconjugate or free LPMO corresponding to a final enzyme concentration of 1.03 μM for *Ls*AA9A variants or 0.23 μM for *Sc*AA10C variants in 50 mM Bis-Tris, pH 6.5, for *Ls*AA9A variants, or 50 mM Tris-HCl, pH 7.5, for *Sc*AA10C variants. The amount of protein present in the bioconjugates was estimated from the SDS-PAGE based quantification described above. The reaction mixtures were incubated at 30 °C for 5 minutes, then the reaction was initiated with the addition of 1 mM ascorbate. The production of the coloured product resorufin was monitored at 540 nm over time using a Multiskan FC microplate photometer (Thermo Fisher Scientific, Waltham, MA, USA), and rates were derived from the initial linear part of the progress curves. A hydrogen peroxide standard curve was prepared in a similar manner, with ascorbate added prior to the addition of Amplex Red and HRP. Thus, the concentration of hydrogen peroxide was calculated after adjusting for side-reactions between ascorbate and oxidised Amplex Red[34].

Peroxidase activity. The peroxidase activity of the LPMOs was assessed by measuring the oxidation of 2,6-dimethoxyphenol (2,6-DMP) based on a protocol by Breslmayr *et al.,* (2018)[36]. Stock solutions of 2,6-DMP (100 mM) were prepared in distilled water. 1 mM 2,6-DMP was reacted with 100 μM hydrogen peroxide and an amount of bioconjugate or free LPMO corresponding to a final enzyme concentration of 1.03 μM for *Ls*AA9A variants or 0.23 μM for *Sc*AA10C variants in 50 mM Bis-Tris, pH 6.5, for *Ls*AA9A variants, or 50 mM Tris-HCl, pH 7.5, for *Sc*AA10C variants. The amount of protein present in the bioconjugates was estimated from the SDS-PAGE based quantification described above. Reactions were initiated with the addition of the LPMO and incubated at 30 °C. The production of the coloured product coerulignone was monitored at 469 nm over time using a Multiskan™ FC microplate photometer (Thermo Fisher Scientific, Waltham, MA, USA), and rates were derived from the initial linear part of the progress curves.

Catalytic assay to evaluate the formation of oxidised products. For *Ls*AA9A variants the formation of C4-oxidised products (Glc4gemGlc and Glc4gemGlc$_2$) was measured. 1 mM cellopentaose or 0.1% (w/v) PASC or 1% (w/v) Avicel, in 50 mM Bis-Tris, pH 6.5, was reacted with an amount of bioconjugate or free *Ls*AA9A variant corresponding to a final enzyme concentration of 1.03 μM. Reactions were initiated with the addition of 1 mM ascorbate and were incubated at 37 °C, 1,000 rpm, in an Eppendorf ThermoMixer C (Eppendorf, Hamburg, Germany). Samples were taken over a 24-hour period and the reactions were stopped by incubating at 100 °C for 15 minutes to inactivate the protein, after which the samples were filtered through a 0.45 μm 96-well filter plate (Millipore, Burlington, MA). For *Sc*AA10C variants the formation of C1-oxidised products was measured. 0.1% (w/v) PASC or 1% (w/v) Avicel, in 50 mM Tris, pH 7.5, was reacted with an amount of bioconjugate or free *Sc*AA10C variant corresponding to a final enzyme concentration of 0.23 μM. Reactions were initiated with the addition of 1 mM ascorbate and incubated at 40 °C, 1000 rpm, in an Eppendorf ThermoMixer C (Eppendorf, Hamburg, Germany). Samples were taken over a 24-hour period and the reactions were stopped by filtering the sample through a 0.45 μm 96-well filter plate (Millipore, Burlington, MA) to separate the insoluble substrate from the LPMO.

Product quantification: Prior to analysis, samples derived from *Sc*AA10C variant reactions were treated with 1 μM of an endoglucanase from *Thermobifida fusca* (*Tf*Cel6A;[45]) at 37 °C, overnight, to convert longer oligomeric C1-oxidised products to a mixture of oxidised dimers (GlcGlc1A)

and trimers (Glc_2Glc1A), allowing for easier quantification. *Ls*AA9A is active on longer soluble products and as a result only the C4-oxidised dimer (Glc4gemGlc) and trimer ($Glc4gemGlc_2$) accumulate, alleviating the need for further processing prior to product analysis and quantification. Quantification of the C1- and C4-oxidised products was performed using high performance anion exchange chromatography with pulsed amperometric detection (HPAEC-PAD), as previously described[46]. HPAEC-PAD was performed on a Dionex ICS6000 (Thermo Fisher Scientific, Waltham, MA) equipped with a 1 × 250 nm Dionex CarboPac PA-200 analytical column attached to 1 × 50 nm Dionex CarboPac PA-200 guard column. The operational flow was 63 µL/min, and 4 µL samples were injected. Eluent generator cartridges were used containing KMSA and KOH. A 26-minute method was used for analysing C1-oxidised products while a longer 45-minute method was used when analysing C4-oxidised products. For details of the gradients used see Østby *et al.,* (2022)[46]. Quantification was performed using standards of C1- and C4-oxidised cellobiose and cellotriose, which were produced in-house. The C1-oxidised standards were produced by incubating 0.5 mM native cellobiose or cellotriose (Megazyme, Bray, Ireland) with 2 µM cellobiose dehydrogenase from *Myriococcum thermophilum* (*Mt*CDH), also produced in-house[47]. The C4-oxidised standards were produced by incubating 3 mM cellopentaose (Megazyme, Bray, Ireland) with 2 µM *Nc*AA9C and 2 mM ascorbate in 10 mM Tris-HCl, pH 8.0, overnight at 33 °C overnight as described previously[48].

Assessing oxidative damage: The same concentrations and conditions were used as described above, but the order of the reagents added to the reaction differed. First, LPMO, buffer and 1 mM ascorbate were incubated for various time periods (5-120 minutes), then the appropriate substrate and an additional 1 mM ascorbate were added to initiate the reaction. The additional ascorbate was added to account for any ascorbate consumption during the pre-incubation. The reactions were incubated for 24-hours and then stopped as described as above.

ASSOCIATED CONTENT

Supplementary material.

This manuscript has supplementary material.

AUTHOR INFORMATION

Author Contributions

The manuscript was written through contributions of all authors. All authors have given approval to the final version of the manuscript. ‡These authors contributed equally. (match statement to author names with a symbol)

Data management

Research data can be shared upon request.

Funding Sources

This work was funded by the European Research Council (ERC) through the Horizon 2020 synergy project CUBE (Unraveling the secrets of Cu-based catalysts for C-H bond activation), grant number 856446.

Acknowledgment

This work was funded by the European Research Council (ERC) through the Horizon 2020 synergy project CUBE (Unraveling the secrets of Cu-based catalysts for C-H bond activation), grant number 856446.

C.P., F.C., M.B., C.B. and S.B. acknowledge support from the Project CH4.0 under the MUR program “Dipartimenti di Eccellenza 2023–2027" (CUP: D13C22003520001)

References

(1) Vaaje-Kolstad, G.; Houston, D. R.; Riemen, A. H.; Eijsink, V. G. H.; van Aalten, D. M. Crystal structure and binding properties of the *Serratia marcescens* chitin-binding protein CBP21. *J. Biol. Chem.* **2005**, *280*, 11313-11319.

(2) Vaaje-Kolstad, G.; Westereng, B.; Horn, S. J.; Liu, Z.; Zhai, H.; Sørlie, M.; Eijsink, V. G. H. An oxidative enzyme boosting the enzymatic conversion of recalcitrant polysaccharides. *Science* **2010**, *330*, 219-222.

(3) Quinlan, R. J.; Sweeney, M. D.; Lo Leggio, L.; Otten, H.; Poulsen, J. C. N.; Johansen, K. S.; Krogh, K. B. R. M.; Jorgensen, C. I.; Tovborg, M.; Anthonsen, A.; Tryfona, T.; Walter, C. P.; Dupree, P.; Xu, F.; Davies, G. J.; Walton, P. H. Insights into the oxidative degradation of cellulose by a copper metalloenzyme that exploits biomass components. *Proc. Natl. Acad. Sci. USA* **2011**, *108*, 15079-15084.

(4) Phillips, C. M.; Beeson, W. T.; Cate, J. H.; Marletta, M. A. Cellobiose dehydrogenase and a copper-dependent polysaccharide monooxygenase potentiate cellulose degradation by *Neurospora crassa*. *ACS Chem. Biol.* **2011**, *6*, 1399-1406.

(5) Munzone, A.; Eijsink, V. G. H.; Berrin, J. G.; Bissaro, B. Expanding the catalytic landscape of metalloenzymes with lytic polysaccharide monooxygenases. *Nat. Rev. Chem.* **2024**, *8*, 106-119.

(6) Bissaro, B.; Røhr, Å. K.; Müller, G.; Chylenski, P.; Skaugen, M.; Forsberg, Z.; Horn, S. J.; Vaaje-Kolstad, G.; Eijsink, V. G. H. Oxidative cleavage of polysaccharides by monocopper enzymes depends on H_2O_2. *Nat. Chem. Biol.* **2017**, *13*, 1123-1128.

(7) Frommhagen, M.; Koetsier, M. J.; Westphal, A. H.; Visser, J.; Hinz, S. W.; Vincken, J. P.; van Berkel, W. J.; Kabel, M. A.; Gruppen, H. Lytic polysaccharide monooxygenases from *Myceliophthora thermophila* C1 differ in substrate preference and reducing agent specificity. *Biotechnol. Biofuels* **2016**, *9*, 186.

(8) Kracher, D.; Scheiblbrandner, S.; Felice, A. K.; Breslmayr, E.; Preims, M.; Ludwicka, K.; Haltrich, D.; Eijsink, V. G.; Ludwig, R. Extracellular electron transfer systems fuel cellulose oxidative degradation. *Science* **2016**, *352*, 1098-1101.

(9) Garajova, S.; Mathieu, Y.; Beccia, M. R.; Bennati-Granier, C.; Biaso, F.; Fanuel, M.; Ropartz, D.; Guigliarelli, B.; Record, E.; Rogniaux, H.; Henrissat, B.; Berrin, J. G. Single-domain flavoenzymes trigger lytic polysaccharide monooxygenases for oxidative degradation of cellulose. *Sci. Rep.* **2016**, *6*, 28276.

(10) Langston, J. A.; Shaghasi, T.; Abbate, E.; Xu, F.; Vlasenko, E.; Sweeney, M. D. Oxidoreductive cellulose depolymerization by the enzymes cellobiose dehydrogenase and glycoside hydrolase 61. *Appl. Environ. Microbiol.* **2011**, *77*, 7007-7015.

(11) Cannella, D.; Hsieh, C. W. C.; Felby, C.; Jorgensen, H. Production and effect of aldonic acids during enzymatic hydrolysis of lignocellulose at high dry matter content. *Biotechnol. Biofuels* **2012**, *5*, 26.

(12) Østby, H.; Hansen, L. D.; Horn, S. J.; Eijsink, V. G. H.; Várnai, A. Enzymatic processing of lignocellulosic biomass: principles, recent advances and perspectives. *J. Ind. Microbiol. Biotechnol.* **2020**, *47*, 623-657.

(13) Bouchey, C. J.; Shopov, D. Y.; Gruen, A. D.; Tolman, W. B. Mimicking the Cu active site of lytic polysaccharide monooxygenase using monoanionic tridentate N-donor ligands. *ACS Omega* **2022**, *7*, 35217-35232.

(14) Kim, B.; Brueggemeyer, M. T.; Transue, W. J.; Park, Y.; Cho, J.; Siegler, M. A.; Solomon, E. I.; Karlin, K. D. Fenton-like chemistry by a copper(I) complex and H_2O_2 relevant to enzyme peroxygenase C-H hydroxylation. *J. Am. Chem. Soc.* **2023**, *145*, 11735-11744.

(15) Kracher, D.; Andlar, M.; Furtmuller, P. G.; Ludwig, R. Active-site copper reduction promotes substrate binding of fungal lytic polysaccharide monooxygenase and reduces stability. *J. Biol. Chem.* **2018**, *293*, 1676-1687.

(16) Courtade, G.; Forsberg, Z.; Heggset, E. B.; Eijsink, V. G. H.; Aachmann, F. L. The carbohydrate-binding module and linker of a modular lytic polysaccharide monooxygenase promote localized cellulose oxidation. *J. Biol. Chem.* **2018**, *293*, 13006-13015.

(17) Stepnov, A. A.; Eijsink, V. G. H.; Forsberg, Z. Enhanced in situ H_2O_2 production explains synergy between an LPMO with a cellulose-binding domain and a single-domain LPMO. *Sci. Rep.* **2022**, *12*, 6129.

(18) Bernal, C.; Rodriguez, K.; Martinez, R. Integrating enzyme immobilization and protein engineering: An alternative path for the development of novel and improved industrial biocatalysts. *Biotechnol. Adv.* **2018**, *36*, 1470-1480.

(19) Homaei, A. A.; Sariri, R.; Vianello, F.; Stevanato, R. Enzyme immobilization: an update. *J. Chem. Biol.* **2013**, *6*, 185-205.

(20) Datta, S.; Christena, L. R.; Rajaram, Y. R. Enzyme immobilization: an overview on techniques and support materials. *3 Biotech.* **2013**, *3*, 1-9.

(21) Singh, N.; Dhanya, B. S.; Verma, M. L. Nano-immobilized biocatalysts and their potential biotechnological applications in bioenergy production. *Mater. Sci. Energy. Technol.* **2020**, *3*, 808-824.

(22) Basso, A.; Serban, S. Industrial applications of immobilized enzymes - a review. *Mol. Catal.* **2019**, *479*, 110607.

(23) Bilal, M.; Nguyen, T. A.; Iqbal, H. M. N. Multifunctional carbon nanotubes and their derived nano-constructs for enzyme immobilization - A paradigm shift in biocatalyst design. *Coord. Chem. Rev.* **2020**, *422*, 213475.

(24) Ijaz, H.; Mahmood, A.; Abdel-Daim, M. M.; Sarfraz, R. M.; Zaman, M.; Zafar, N.; Alshehery, S.; Salem-Bekhit, M. M.; Ali, M. A.; Eltayeb, L. B.; Benguerba, Y. Review on carbon nanotubes (CNTs) and their chemical and physical characteristics, with particular emphasis on potential applications in biomedicine. *Inorg. Chem. Commun.* **2023**, *155*, 111020.

(25) Li, J.; Pandey, G. P. Advanced physical chemistry of carbon nanotubes. *Annu. Rev. Phys. Chem.* **2015**, *66*, 331-356.

(26) Mezzasalma, S. A.; Grassi, L.; Grassi, M. Physical and chemical properties of carbon nanotubes in view of mechanistic neuroscience investigations. Some outlook from condensed matter, materials science and physical chemistry. *Mater. Sci. Eng. C* **2021**, *131*, 112480.

(27) Pagolu, R.; Singh, R.; Shanmugam, R.; Kondaveeti, S.; Patel, S. K. S.; Kalia, V. C.; Lee, J. K. Site-directed lysine modification of xylanase for oriented immobilization onto silicon dioxide nanoparticles. *Bioresour. Technol.* **2021**, *331*, 125063.

(28) Mubarak, N. M.; Wong, J. R.; Tan, K. W.; Sahu, J. N.; Abdullah, E. C.; Jayakumar, N. S.; Ganesan, P. Immobilization of cellulase enzyme on functionalized multiwall carbon nanotubes. *J. Mol. Catal. B Enzym.* **2014**, *107*, 124-131.

(29) Alagöz, D.; Toprak, A.; Yildirim, D.; Tukel, S. S.; Fernandez-Lafuente, R. Modified silicates and carbon nanotubes for immobilization of lipase from *Rhizomucor miehei*: Effect of support and immobilization technique on the catalytic performance of the immobilized biocatalysts. *Enzyme Microb. Technol.* **2021**, *144*, 109739.

(30) Jiang, K.; Schadler, L. S.; Siegel, R. W.; Zhang, X.; Zhang, H.; Terrones, M. Protein immobilization on carbon nanotubes via a two-step process of diimide-activated amidation. *J. Mater. Chem.* **2004**, *14*, 37-39.

(31) Vaaje-Kolstad, G.; Forsberg, Z.; Loose, J. S.; Bissaro, B.; Eijsink, V. G. Structural diversity of lytic polysaccharide monooxygenases. *Curr. Opin. Struct. Biol.* **2017**, *44*, 67-76.

(32) Schneider, C. A.; Rasband, W. S.; Eliceiri, K. W. NIH Image to ImageJ: 25 years of image analysis. *Nat. Methods* **2012**, *9*, 671-675.

(33) Kittl, R.; Kracher, D.; Burgstaller, D.; Haltrich, D.; Ludwig, R. Production of four *Neurospora crassa* lytic polysaccharide monooxygenases in *Pichia pastoris* monitored by a fluorimetric assay. *Biotechnol. Biofuels* **2012**, *5*, 79.

(34) Stepnov, A. A.; Eijsink, V. G. H. Looking at LPMO reactions through the lens of the HRP/amplex red assay. *Methods Enzymol.* **2023**, *679*, 163-189.

(35) Rieder, L.; Stepnov, A. A.; Sørlie, M.; Eijsink, V. G. H. Fast and specific peroxygenase reactions catalyzed by fungal mono-copper enzymes. *Biochem.* **2021**, *60*, 3633-3643.

(36) Breslmayr, E.; Hanzek, M.; Hanrahan, A.; Leitner, C.; Kittl, R.; Santek, B.; Oostenbrink, C.; Ludwig, R. A fast and sensitive activity assay for lytic polysaccharide monooxygenase. *Biotechnol. Biofuels* **2018**, *11*, 79.

(37) Votvik, A. K.; Røhr, Å. K.; Bissaro, B.; Stepnov, A. A.; Sørlie, M.; Eijsink, V. G. H.; Forsberg, Z. Structural and functional characterization of the catalytic domain of a cell-wall anchored bacterial lytic polysaccharide monooxygenase from *Streptomyces coelicolor*. *Sci. Rep.* **2023**, *13*, 5345.

(38) Zhou, P.; Zhang, J.; Zhang, Y.; Liu, Y.; Liang, J.; Liua, B.; Zhang, W. Generation of hydrogen peroxide and hydroxyl radical resulting from oxygen-dependent oxidation of L-ascorbic acid via copper redox-catalyzed reactions. *RCS Adv.* **2016**, *6*, 38541-38547.

(39) Stepnov, A. A.; Forsberg, Z.; Sørlie, M.; Nguyen, G. S.; Wentzel, A.; Røhr, Å. K.; Eijsink, V. G. H. Unraveling the roles of the reductant and free copper ions in LPMO kinetics. *Biotechnol. Biofuels* **2021**, *14*, 28.

(40) Rieder, L.; Ebner, K.; Glieder, A.; Sørlie, M. Novel molecular biological tools for the efficient expression of fungal lytic polysaccharide monooxygenases in *Pichia pastoris*. *Biotechnol. Biofuels* **2021**, *14*, 122.

(41) Forsberg, Z.; Mackenzie, A. K.; Sørlie, M.; Røhr, Å. K.; Helland, R.; Arvai, A. S.; Vaaje-Kolstad, G.; Eijsink, V. G. Structural and functional characterization of a conserved pair of bacterial cellulose-oxidizing lytic polysaccharide monooxygenases. *Proc. Natl. Acad. Sci. U.S.A.* **2014**, *111*, 8446-8451.

(42) Forsberg, Z.; Røhr, Å. K.; Mekasha, S.; Andersson, K. K.; Eijsink, V. G.; Vaaje-Kolstad, G.; Sørlie, M. Comparative study of two chitin-active and two cellulose-active AA10-type lytic polysaccharide monooxygenases. *Biochemistry* **2014**, *53*, 1647-1656.

(43) Manoil, C.; Beckwith, J. A genetic approach to analyzing membrane protein topology. *Science* **1986**, *233*, 1403-1408.

(44) Wilkins, M. R.; Gasteiger, E.; Bairoch, A.; Sanchez, J. C.; Williams, K. L.; Appel, R. D.; Hochstrasser, D. F. Protein identification and analysis tools in the ExPASy server. *Methods Mol. Biol.* **1999**, *112*, 531-552.

(45) Calza, R. E.; Irwin, D. C.; Wilson, D. B. Purification and characterization of two β-1,4-endoglucanases from *Thermomonospora fusca*. *Biochemistry* **1985**, *24*, 7797-7804.

(46) Østby, H.; Jameson, J. K.; Costa, T.; Eijsink, V. G. H.; Arntzen, M. O. Chromatographic analysis of oxidized cello-oligomers generated by lytic polysaccharide monooxygenases using dual electrolytic eluent generation. *J. Chromatogr. A* **2022**, *1662*, 462691.

(47) Zamocky, M.; Schumann, C.; Sygmund, C.; O'Callaghan, J.; Dobson, A. D.; Ludwig, R.; Haltrich, D.; Peterbauer, C. K. Cloning, sequence analysis and heterologous expression in *Pichia pastoris* of a gene encoding a thermostable cellobiose dehydrogenase from *Myriococcum thermophilum*. *Protein Expr. Purif.* **2008**, *59*, 258-265.

(48) Müller, G.; Várnai, A.; Johansen, K. S.; Eijsink, V. G.; Horn, S. J. Harnessing the potential of LPMO-containing cellulase cocktails poses new demands on processing conditions. *Biotechnol. Biofuels* **2015**, *8*, 187.

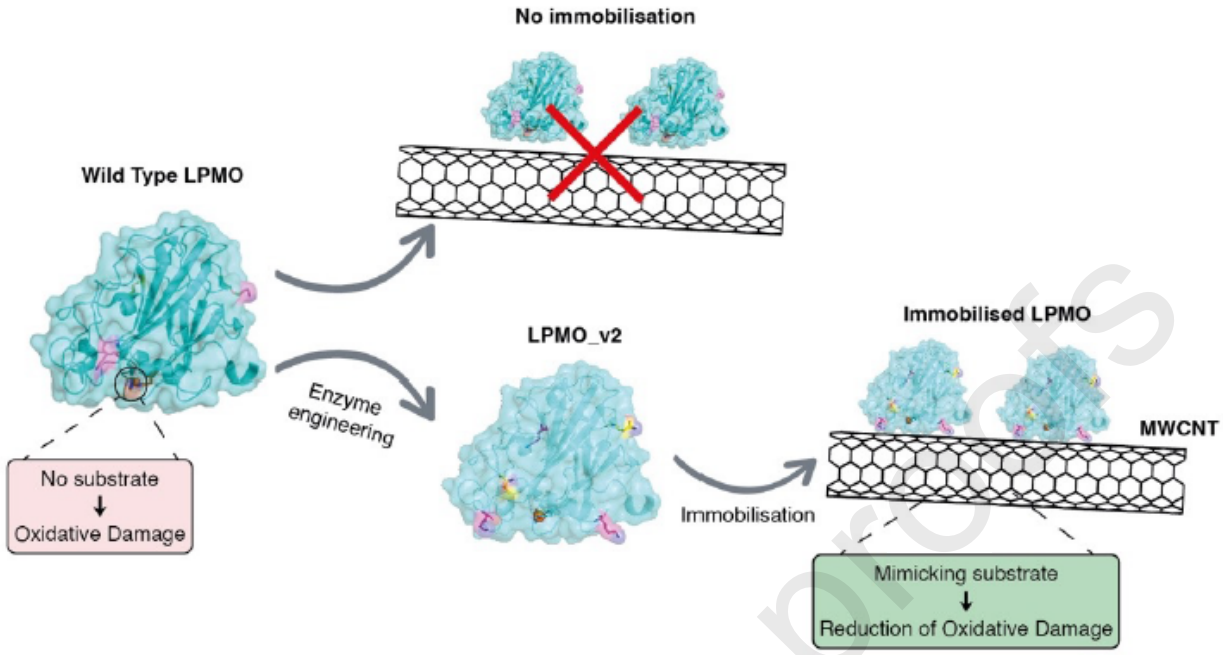

Highlights

- Covalent immobilization of lytic polysaccharide monooxygenases on carbon nanotubes.
- Site-mutations to improve specific orientation of enzyme on immobilization.
- Catalytic activity is retained.
- Enhanced stability against oxidative self-inactivation.

Declaration of Interest Statement

The authors declare no conflicts of interests.